Proceedings of the 15th International Heat Transfer Conference, IHTC-15
August 10-15, 2014, Kyoto, Japan

IHTC15-9662

REGIMES OF HEATING AND COMPRESSION IN MAGNETO-INERTIAL FUSION

Victor V. Kuzenov[1,2], Sergei V. Ryzhkov[1*]

[1]Bauman Moscow State Technical University, 2nd Baumanskaya Street, bld.5, str. 1
Moscow 105005, Russia
[2]A.Yu. Ishlinsky Institute for Problems in Mechanics RAS, prosp. Vernadskogo 101, block 1
Moscow 119526, Russia

ABSTRACT

Simulation models of ignition and burn for magnetized fuel target compressed by high pulse energy lasers (laser driver) and high velocity plasma guns (plasma liner) are presented. An improved radiation-hydrodynamics code FUCUS (Fusion bUrn in targets under Compression nUmerical Simulation) which simulates plasmas in cylindrical or spherical geometries is created. Numerical method to determine parameters and regimes in a mathematical model of magnetized target plasma compression and heating is described. Models for high pulse energy laser, high speed plasma jets and magnetic field are presented. The method of quasi-mechanical analogy is used to build the regular adaptive grid. Different regimes in the target for magneto-inertial fusion are considered. The effect of external magnetic field on the radiation-magnetic hydrodynamic instabilities is discussed.

KEY WORDS: Computational methods, Radiation, Magnetized target, Laser beams, Plasma jets

1. INTRODUCTION

The concept of fast ignition is one of the most promising approaches to the problem of controlled fusion. It is based on the principle of separation with respect to time of the target compression (first regime is a slow adiabatic compression of the thermonuclear target) and the process of thermonuclear ignition of a deuterium-tritium (*D-T*) mixture (second regime is rapid heating of a target and thermonuclear combustion wave initiation in the small target area). Such an approach allows reducing the energy needed to start a *D-T* fusion reaction: 20 - 50 kJ for the ignition threshold and 0.3 - 1 MJ for the initiation of high gain fusion.

In this paper the scheme of magneto-inertial fusion (MIF) [1-7] is applied for the first stage of "fast ignition". MIF has the advantages of both concepts: controlled thermonuclear fusion - high energy density (typical for inertial confinement fusion) and the thermal insulation of plasma by the magnetic field (typical for magnetic confinement fusion). The scheme of laser-driven MIF is based on the general idea of adiabatic acceleration (compression and heating) of the magnetized target by high pulse energy laser. The target consists of a pre-formed low-temperature plasma and is "frozen" into the plasma magnetic field.

The generation of initial “seed” magnetic field is required before laser is put into effect. Further, the fusion target must be "evenly" irradiated by multi-channel laser. As a result of the target surface interaction with heat radiation a hot plasma is formed with a temperature $T = 1 \div 5$ keV. The so-called plasma corona expanding with typical speed $u = 10^2 \div 10^3$ km/s and creating a compressive pressure $P \approx 5 \times 10^7$ bar. In this case, the laser-induced heat radiation penetrates into the target center until the critical electron density (frequency of the laser radiation is of the same order of magnitude as the plasma frequency) is achieved. The

*Corresponding Author: ryzhkov@power.bmstu.ru

reflection of laser light from the border with the critical electron density is an important problem facing laser inertial fusion.

Only a brief summary of the models will be included in the present paper. Section 2 describes the mathematical models for high speed plasma jets used in the present analysis. Section 3 sets up equations for the magnetic field in an adaptive curvilinear coordinate system. Section 4 deals with radiation-magnetic hydrodynamic instabilities such as Rayleigh–Taylor (RTI) and Richtmyer–Meshkov (RMI), and the associated turbulent mixing. The presence of hydrodynamic instabilities is one of the main obstacles in the way of solving ICF problem. The final section summarizes and draws conclusions. Energies are expressed in SI units and temperatures - in keV.

2. ZERO-DIMENSIONAL MATHEMATICAL MODEL FOR PULSED PLASMA JETS

We developed a mathematical model of the electrodynamic method to describe the compression and heating of the magnetized plasma (fusion target) by high speed plasma jets (plasma liner).

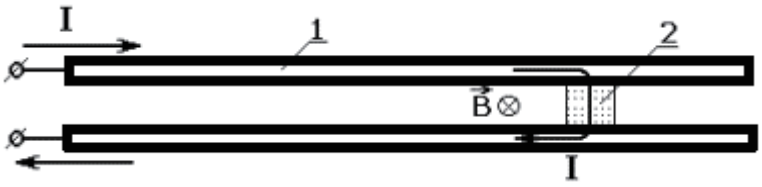

Fig. 1 A schematic of the railgun accelerator: 1 - electrodes ("rails"), 2 – plasma, I is the current.

We consider two types of pulsed electromagnetic plasma accelerators:
1) a plasma railgun (Fig. 1) which is "supplied" from the capacitive energy storage device and has a rectangular channel cross section of the accelerator. A plasmoid can be created either by erosion of the dielectric insert under the influence of sliding discharge or by the plasma injection of additional discharge channel. Electrodynamic acceleration of the quasi-neutral plasma of small size is based on the Ampere's law of the interaction of the magnetic field and a current carrying conductor;
2) a pulsed coaxial accelerator (Fig. 2) working with gas or products of ~~an~~ erosion of a dielectric interelectrode insert and which has cylindrical cross sections of the accelerator channel. The physics of plasma acceleration is similar to dynamics of acceleration in a railgun channel. Accelerators of this kind (hydrogen is used as a working substance) allow receiving streams with speeds of ~10^8 cm/s (10 keV / a particle) with the total energy content of the system ~ 1 MJ (~10^{22} particles/pulse) [8-11].

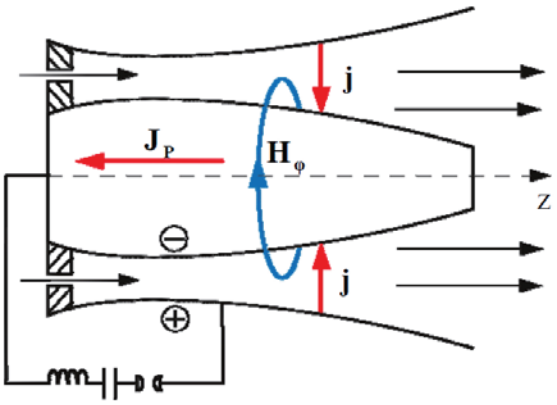

Fig. 2 Coaxial plasma accelerator schematic.

The following parameters for compressible flow were obtained in present-day devices: generation time 2 - 10 μs; density $n \approx 10^{14} \div 10^{19}$ cm^{-3}, speed $v \approx 10^{6} \div 10^{8}$ cm/s, ion temperature ~ 1 keV (~ 10^{7} K); total energy flux density $q \approx 10^{15}$ W/cm^{2}.

The plasma cluster will act like as a rigid bridge (it is assumed that the turbulent mixing of the plasma and the environment is not substantial and $dm/dt = 0$) in the zero-dimensional electrodynamics [12, 13]. The same mathematical model of the plasma acceleration process can be used for both railgun and pulsed coaxial accelerator. In this approximation, the process is described by the following equations in coordinates (t, z)

$$m\frac{d^2z}{dt^2} = F\,,\ F = \frac{J^2}{2}\frac{dL}{dz}\,,\ J = -C_0\frac{dU}{dt}\,,\ L = L_0 + \ell z\,,$$

$$\frac{d(LJ)}{dt} + RJ - U = 0 \ \text{ or } \ C_0L_0\frac{d}{dt}\left[\left(1 + \frac{\ell}{L_0}z\right)\frac{dU}{dt}\right] + RC_0\frac{dU}{dt} + U = 0\,,$$

$$\text{at } t = 0\text{: } dz/dt = 0,\ z = 0,\ J = 0,\ U = U_0,$$

where t is the time, J is the current in the circuit at arbitrary time, U_0 is the starting voltage between electrodes, U is the voltage between the electrodes at arbitrary time, $R = R_0 + R_{pl}$ is the resistance of lead wires R_0 and plasma bridge circuit R_{pl}, C_0 is the capacity of the capacitor bank, L_0 is the initial inductance of the circuit, ℓ is the dispersed inductance of a circuit, L is the full inductance of a circuit, $m = m_0$ is the initial mass.

For the pulsed accelerators the following values of electrical parameters are common: $U_0 \approx (1 \div 100) \times 10^{3}$ V, $R_0 \approx (10^{-1} \div 10^{-3})$ Ohm, $R_{pl} \approx 10^{-3}$ Ohm, $C_0 \approx (10 \div 200) \times 10^{-6}$ F, $L_0 \approx (50 \div 100) \times 10^{-9}$ H, $l_0 \approx (0{,}1 \div 10) \times 10^{-7}$ H/m, $m \approx (1 \div 20)\ \mu$g.

The resistance of plasma is given by (ψ=1 for the surface discharge or pulsed plasma accelerator):

$$R_{pl} = L/(\psi b\int_0^{\ell}\sigma(z)dz)\,.$$

These equations and initial conditions depend on two dimensionless parameters $q_1 = \dfrac{\ell^2C_0^2U_0^2}{2m_0L_0}$, $q_2 = RC_0\omega_0$ and can therefore be represented by dimensionless variables:

$$\tilde{z} = \frac{\ell}{L_0}z\,,\ \widetilde{U} = \frac{U}{U_0}\,,\ \tilde{t} = \omega_0 t\,,\ \omega_0 = \frac{1}{\sqrt{L_0C_0}}\,,\ \widetilde{m} = \frac{m}{m_0}\,,$$

$$\frac{d^2\tilde{z}}{d\tilde{t}^2} = q_1\left(\frac{d\widetilde{U}}{d\tilde{t}}\right)^2\,,\ \frac{d}{d\tilde{t}}\left[\left(1 + \tilde{z}\right)\frac{d\widetilde{U}}{d\tilde{t}}\right] + q_2\frac{d\widetilde{U}}{d\tilde{t}} = -\widetilde{U}\,,$$

$$\tilde{z}\left(0\right) = 0\,,\ \left.\frac{d\tilde{z}}{d\tilde{t}}\right|_{\tilde{t}=0} = 0\,,\ \widetilde{U}\left(0\right) = 1\,,\ \left.\frac{d\widetilde{U}}{d\tilde{t}}\right|_{\tilde{t}=0} = 0\,.$$

It is necessary to determine the values of electrical parameters U_0, R_0, R_{pl}, C_0, L_0, ℓ_0, m for the mathematical description of the pulsed plasma accelerator. The expression for the magnetic energy in the gap between the electrodes is: $W\left(z\right) = \mu\int\dfrac{H^2}{2}dV$, where $\mu = 4\pi\cdot10^{-7}\ \dfrac{\text{H}}{\text{m}}$ is the magnetic permeability of vacuum, V is the volume of the interelectrode gap occupied with magnetic field. The inductance of a coaxial pulsed plasma accelerator $L(t)$ can be found from the energy ratio $W = LJ^2/2$ and the condition that the magnetic field in the

gap between the electrodes of accelerator is determined by the law $H = J / 2\pi r$, where J is the current, flowing between the electrodes, $r(x,y) = \sqrt{x^2 + y^2}$.

Then the coefficient of induction for coaxial accelerator and the inductance per unit length ℓ [13] are:

$$\ell z = \frac{\mu J^2}{4\pi} \ln\left(\frac{R_2}{R_1}\right) z \,,\ \ell = \frac{\mu J^2}{4\pi} \ln\left(\frac{R_2}{R_1}\right),$$

where R_2, R_1 are the radii of the central and outer electrodes, respectively. The inductance per unit length for the two wire electrodes of diameter D at a distance S from each other: $\ell = \frac{\mu}{\pi} Arch\left(\frac{s}{D}\right)$.

However, the experimental [15] and theoretical studies [14] allow us to say that thermal parameters of gases have a significant effect on the plasmoid acceleration. Therefore, for example, the maximum speed of the plasma piston has a limit due to the resistance of the environment and the reduction of plasma acceleration when the vaporized electrode material is involved in the movement [15]. We assume that the mass of the accelerated plasma is changed by the electrode ablation undergoing its own broadband radiation. The braking of plasmoids is carried out by the pressure of the surrounding gas compressed in the bow shock. In this case, an approach to electrodynamics is modified and takes the form:

$$m\frac{d^2 z}{dt^2} + \left(\frac{dm}{dt}\right)\frac{dz}{dt} = F \,,\ F = \frac{J^2}{2}\frac{dL}{dz} - p_2 F \,,\ \frac{dm}{dt} = \alpha J^2 \,,$$

where p_2 is the pressure of the gas behind a shock wave front, moving ahead of the plasma in a stationary gas at an arbitrary time, α is the ablation parameter that takes into account the mass, involved in the movement along with the accelerated plasma, F is the cross sectional area of the accelerated plasma cluster mass m. The coefficient α slightly depends on the current size $\alpha \approx (2 \div 5) \times 10^{-12}$ kg/(A^2·s) for $J \geq 300$ kA [16].

The ratio for the strong ($p_2 \gg p_1$) shock wave expression is followed by:

$$p_2 F = \frac{1}{1 - \rho_1/\rho_2} \rho_1 F \left(\frac{dz}{dt}\right)^2 = \frac{C}{2} \rho_1 F \left(\frac{dz}{dt}\right)^2 ,$$

where ρ_2 is the density of the surrounding gas and ρ_1 is the density in front of the shock wave.

The equations become more complex after being converted into dimensionless variables:

$$\frac{d^2 \tilde{z}}{d\tilde{t}} + \left(\frac{d\tilde{m}}{d\tilde{t}}\right)\frac{d\tilde{z}}{d\tilde{t}} = q_1 \left(\frac{d\tilde{U}}{d\tilde{t}}\right)^2 - q_3 \left(\frac{d\tilde{z}}{d\tilde{t}}\right)^2 ,\ q_3 = \frac{C}{2}\left(\frac{L_0}{\ell}\omega_0\right)^2 \rho_1 F \,,$$

$$\frac{d\tilde{m}}{d\tilde{t}} = q_4 \left(\frac{d\tilde{U}}{d\tilde{t}}\right)^2 , q_4 = \frac{\alpha\left(C_0 U_0 \omega_0\right)^2}{m_0 \omega_0} .$$

The time of a shock wave formation for the uniform acceleration of the body motion in a continuous medium is known as $t_0 = \frac{2}{\gamma + 1}\frac{c_0}{a_0}$, where c_0 is the speed of sound in the undisturbed environment, a_0 is the initial acceleration of the body. In this case, the shock formation distance of wave is $Z_0 = \frac{a_0 t_0^2}{2} = \frac{2}{(\gamma+1)^2}\frac{c_0^2}{a_0}$.

Numerical estimates [15] show that the formation time of shock waves can be neglected when the resistance force is caused by shock waves. The term $\left(\frac{dm}{dt}\right)\frac{dz}{dt}$, corresponding to a reduced acceleration of plasma cluster because of the vaporization of the electrode material, is the most important factor limiting the speed of the plasma.

In recent years, considerable attention is paid to the development of an electrodynamic accelerator of macrobodies [18-21] with a velocity $v \approx (5 \div 10)$ km/s, and a mass of an accelerated body $m \approx (1 \div 10^3)$ g. Let us note that an electrodynamic approximation to the plasma acceleration process can be directly applied to the description of the acceleration process of macroscopic bodies.

3. INFLUENCE OF EXTERNAL MAGNETIC FIELD ON VORTEX STRUCTURES IN A MODEL OF LASER-DRIVEN IMPLOSION

The equation describing the dynamics of the magnetic field $\vec{B}$ in an adaptive curvilinear coordinate system (ξ,η,ζ) is:

$$\frac{\partial \vec{B}}{\partial t} + \left(\vec{V}_{\xi,\eta,\zeta} \bullet \nabla \vec{B}\right) = rot\left[\vec{V} \times \vec{B}\right] - \frac{c^2}{4\pi} rot\left(\frac{rot\vec{B}}{\sigma}\right).$$

The second term on the left side of the equation is the spontaneous generation of a magnetic field. And the right side contains convective and diffusion components correspondingly.

$$\vec{j} = \sigma\left(\vec{E} + \frac{V_*}{c}\left[\vec{V} \times \vec{B}\right]\right)$$

$$\left(\vec{V}_{\xi,\eta,\zeta} \bullet \nabla \vec{B}\right) = \frac{d\xi}{dt}\frac{\partial \vec{B}}{\partial \xi} + \frac{d\eta}{dt}\frac{\partial \vec{B}}{\partial \eta} + \frac{d\zeta}{dt}\frac{\partial \vec{B}}{\partial \zeta},\ \vec{V}_{\xi,\eta,\zeta} = \left(\frac{d\xi}{dt}, \frac{d\eta}{dt}, \frac{d\zeta}{dt}\right)^T,$$

where σ is the electrical conductivity coefficient, $\vec{E}$ is the intensity of the electric field, and $\vec{V}$ is the plasma velocity.

The developed model [22-24] describes the compression of the target with laser beams in a magnetic field of arbitrary configuration and can be used for numerical study of the formation of plasma in an external seed magnetic field and heating during its compression using high-energy external sources. These equations take into account the compression of the magnetic field frozen into the plasma and the plasma behavior under compression. The Structure of a spontaneous magnetic field in a laser plasma is considered. For laser intensity 10^{18}–10^{20} W/m^2 the main mechanism of generation of spontaneous magnetic fields in a plasma is the thermo-electromagnetic force. In this case the gradient mechanism of magnetic field generation predominates, and the vortex currents are due to non-collinearity of gradients of electron density ∇n_e and temperature ∇T.

An important feature that greatly affects the process of the hydrodynamic instability [24, 25] is the presence in the calculated area of the magnetic field $\vec{B}$, which is defined in the calculations by only one component $\vec{B} = \left(B_x = 0, B_y = 0, B_z = B_0\right)$ perpendicular to the plane of the drawing (Figs. 3 - 5). In this case, the dimensionless parameter depending on the value B_0 is $\beta = 2P_0 / B_0^2$.

The initial constant value of the magnetic field B_0 is given in three ways:
- throughout the estimated area ($B_0 = const$);

- in spatial region between the outer surface of the contact boundary and the calculated boundary of the environment;
- in spatial region between the inner surface of the contact boundary and the calculated boundary of fuel.

The common property of these interactions is that the density of the substance (after shock wave) accelerating metal shell is less than that of the material of the shell itself. Eventually in this case, the instability with the exponential growth of small perturbations may arise between the air (or fuel) and contact boundary. Moreover, during the contact boundary movement conditions for growth on its surface perturbations occur twice: during the acceleration phase and the deceleration step. In the latter case, the perturbations grow on the inner surface of the shell - on its border with fusion fuel.

4. EVALUATION OF THE NONLINEAR HYDRODYNAMIC INSTABILITIES IN INERTIAL CONFINEMENT FUSION TARGET IN A MAGNETIC FIELD

The presence of radiation-magnetic hydrodynamic instabilities on the border between the fusion target and the environment, leads to mixing of cold dense layers of the target material and hot, less dense layers of the environment which leads to a limited amount of energy density achieved in the thermonuclear target (this process markedly worsens conditions for the ignition of thermonuclear reactions). We consider the problem based on a three-layer design area of the turbulent mixing in the two-layer cylindrical targets. As a result, the effect of Mach number on Richtmyer-Meshkov mixing, the amplitude and shape of the initial perturbations, the incident laser intensity on the contact boundary (*CB*) and the impact of magnetic field strength on development of instability and turbulent mixing of the contact boundary can be estimated.

Relatively complex spatial arrangement of the contact boundaries (corresponding to the linear and nonlinear stages of the development of RMI and RTI) shown in Figs. 3-5, are accompanied by a corresponding complex interaction of shock waves, rarefaction waves and contact discontinuities, which can be mathematically described only within multi-dimensional radiation-magnetic Reynolds equations.

To clarify this issue, the problem (based on a three-layer design areas) of turbulent mixing in stratified (double layer) cylindrical targets is considered. The target region in this case is calculated from the following three zones:

• air: ambient gas environment ($\rho_{air} = 1,29 \times 10^{-3}$ g/cm^3);
• thin metal shell, which is presumably made of Be (1,85 g/cm^3), Pb (2,6 g/cm^3), Au (19,3) or Al (2,7 g/cm^3);
• fusion fuel: *D-T* gas (5×10^{-2} g/cm^3).

Thus, in this situation there are two contact boundaries:
• the first contact boundary is located between the environment and the outer surface of the metal shell;
• the second is the contact boundary between the inner surface of the metal shell and fuel.

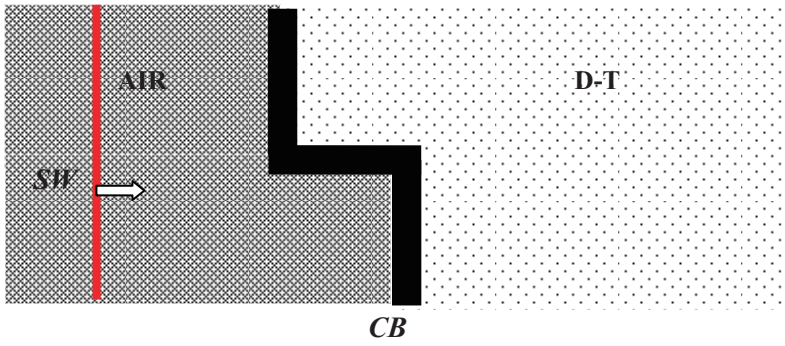

Fig. 3 Shock wave (*SW*) interaction with a graded contact boundary (*CB*) layer of *D-T* target.

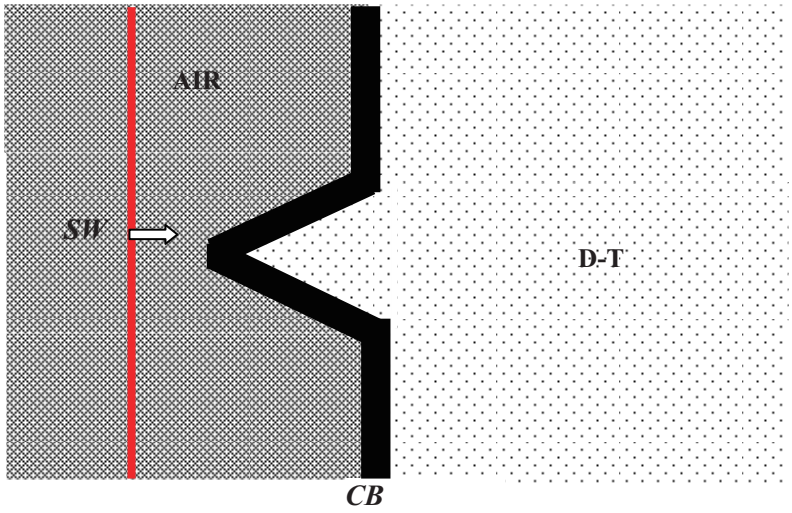

Fig. 4 The fall of the shock wave on the contact boundary: direct angular ledge.

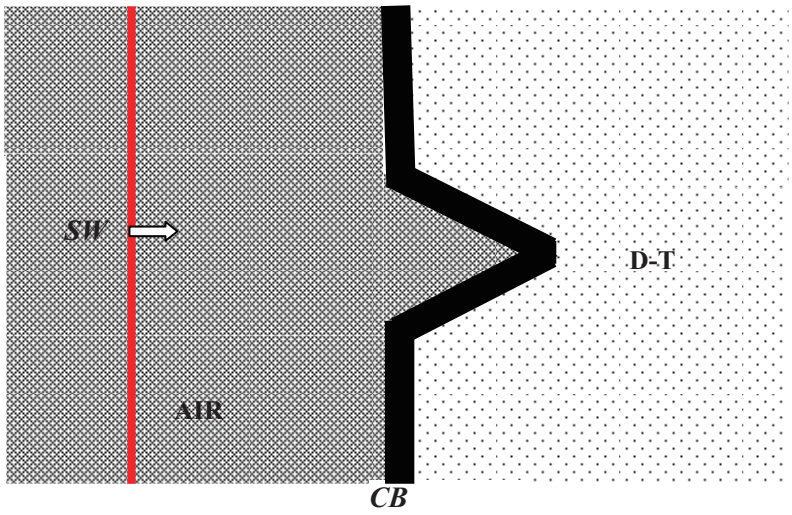

Fig. 5 Schematic representation of simulation scheme: inverse angular ledge.

These boundaries at the initial time have a perspective view of stage (Fig. 3) or angular projection (forward Fig. 4 or reverse Fig. 5) and are perpendicular or at an angle $(\pi/2-\theta)$ to the direction of motion of the shock wave (*SW*). Figs. 3 - 5 show a red shock wave front and its spatial position relative to the contact boundaries (they are arranged perpendicularly or obliquely to the front of the shock wave). The value of the angle θ formed between the shock front and the side of the triangular ledge, are varied in the calculations. Note that a perspective view of the contact boundary conditionally simulates various types of defects in the membrane of fusion target.

For the general description of the radiation-magnetic hydrodynamic instabilities development process the pressure behind the shock front P_0 must be denoted. The effect of the static pressure magnitude on the studied process in the form of the relation: $\mu_p = P/P_0$. The parameter $\mu_p = \mu_p(M)$ for this case is a function of the Mach number M. In the calculations it was assumed that the Mach number is in the range of values 1,3-15. Mach number distribution is shown in Fig. 6.

It is known that Atwood number is used for the evaluation of the development of instabilities with changing the time variable *t*. The Atwood number can be described by a formula such as $A = \frac{(\rho_h - \rho_l)}{(\rho_h + \rho_l)}$, where ρ_h, ρ_l are the densities of the "heavy" and "light" material respectively.

In this version of the problem associated with the development of the RMI and RTI in sandwich settlement areas, for the initial time $t = 0$, it is possible to form two Atwood numbers:

• for the first contact boundary $A_{air} = \frac{(\rho_{CB} - \rho_{Air})}{(\rho_{CB} + \rho_{Air})}$, where ρ_{CB} is in the density of the contact boundary;

• for the area of the second contact boundary $A_{DT} = \frac{(\rho_{CB} - \rho_{DT})}{(\rho_{CB} + \rho_{DT})}$, where ρ_{DT} is the fuel density.

An important geometrical parameter affecting the development of instabilities is the so-called aspect ratio As = R_0/Δ_0, where R_0 is the initial radius of the contact boundary in the cylindrical coordinate system, Δ_0 is the initial thickness of the contact boundary in the cylindrical coordinate system. Two aspect ratios must be set for the geometry of the contact surface: $As_1 = R_0^1 / \Delta_0$ and $As_2 = R_0^2 / \Delta_0$, where R_0^1 is the minimum initial radius of the contact boundary in a cylindrical coordinate system, R_0^2 is the maximum initial radius of the contact boundary in a cylindrical coordinate system.

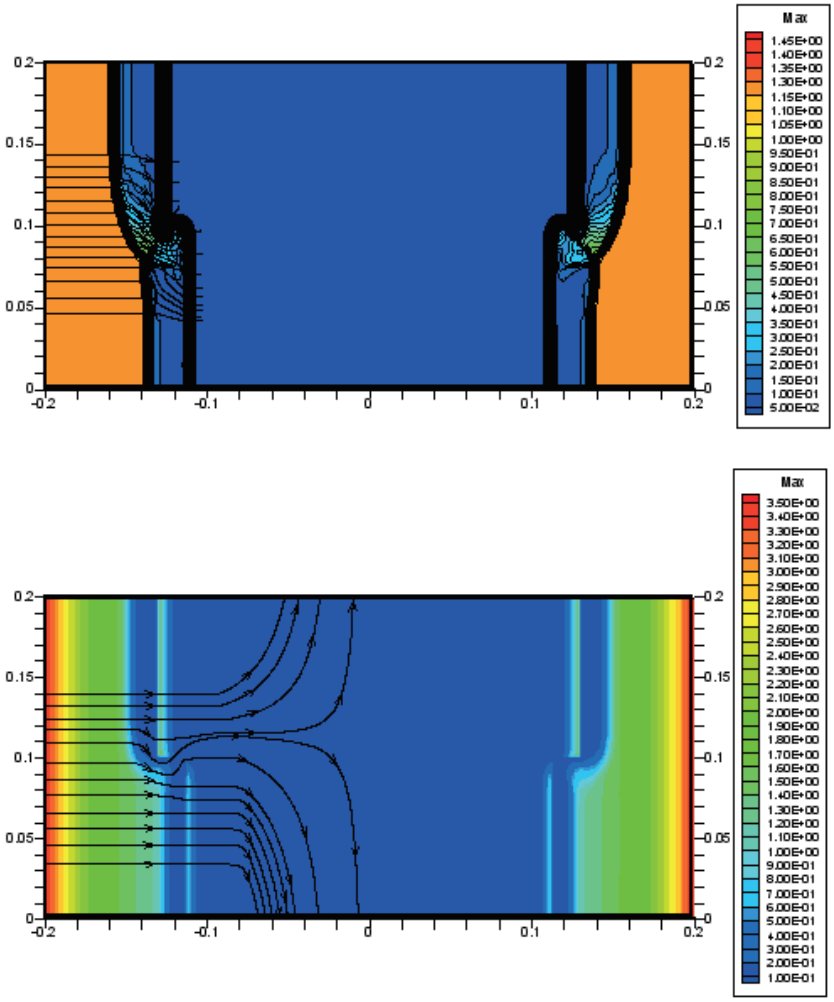

Fig. 6 The spatial distribution of Mach number without a magnetic field (upper picture) and in the presence of a magnetic field (lower picture).

5. CONCLUSIONS

The goal of the investigation is complex numerical research and optimization of the pulsed high-temperature processes in a dense magnetized plasma (target). Distinctive feature of this problem is the presence of initial seed fields (the imposed external pulse magnetic field) and compression of a magnetic flux by laser beams (laser driver). External and spontaneous magnetic fields are taken into account for the so-called magneto-inertial fusion. Laser-driven and plasma jet driven magneto-inertial fusion (MIF) with magnetized target implosion is considered. The condition of thermonuclear ignition of a *D-T* mixture in a magnetic field is significantly attenuated in comparison with conventional inertial and magnetic fusion. Convection, diffusion and generation of spontaneous magnetic field ate taken into account. Two regimes of heating and compression are presented and two stages of slow adiabatic compression and rapid heating of a target are investigated. We introduce the basic dimensionless parameters and two Atwood numbers are formed to define a problem. Mach number distributions are obtained for the different contact boundaries. Modeling of the magnetic field impact on a single plasma jet formed at the laser target compression is performed. It is shown that at the compression and heating of a plasma target by using a rapidly growing external magnetic field and laser radiation the Richtmyer–Meshkov instability can be suppressed.

ACKNOWLEDGMENT

This research was partially supported by the Russian Foundation for Basic Research - RFBR Grant № 13-01-00537; Program of the Presidium of RAS and fundamental research programs of the Department of Energy, Engineering, Mechanics and Control Processes of the RAS; and the Ministry of Education and Science of the Russian Federation (GosZadanie “Scientific and technical basis for the creation of hybrid reactors and systems with powerful heat sources for advanced power systems” № 13.79.2014/K), joint Russian-German "Mikhail Lomonosov” Program (B), 11.9198.2014, and the Rector's Office of the Bauman Moscow State Technical University.

NOMENCLATURE

q	dimensionless variable	(-)	μ_p(M)	function	
ξ	first variable	(-)	As	aspect ratio	
η	second variable	(-)	α	ablation parameter	
ζ	third variable	(-)	β	dimensionless variable	

subscript		superscript	
h	“heavy” material	1	minimum radius
l	“light” material	2	maximum radius
CB	contact boundary	*pl*	plasma

REFERENCES

[1] Gotchev, O.V., Chang, P.Y., Knauer, J.P., Meyerhofer, D.D., Polomarov, O., Frenje, J., Li, C.K., Manuel, M.J.- E., Petrasso, R.D., Rygg, J.R., Seguin, F.H. and Betti, R., “Laser-driven magnetic-flux compression in high-energy-density plasmas,” *Phys. Rev. Lett.*, 103, pp. 215004-4, (2009).

[2] Ryzhkov, S.V. and Anikeev, A.V., “Improved regimes in high pressure magnetic discharges,” *Proc. of 14th Int. Heat Trans. Conf.*, IHTC14-22212, (2010).

[3] Ryzhkov, S.V., “The behavior of a magnetized plasma under the action of laser with high pulse energy,” *Probl. Atom. Sci. Tech.,* 4, pp. 105-110, (2010).

[4] Kostyukov, I.Yu. and Ryzhkov, S.V., “Magneto-Inertial Fusion with Laser Compression of a Magnetized Spherical Target,” *Plasma Phys. Rep.*, 37(13), pp. 1092–1098, (2011).

[5] Ryutov, D.D., Cuneo, M.E., Herrmann, M.C., Sinars, D.B. and Slutz, S.A., "Simulating the magnetized liner inertial fusion plasma confinement with smaller-scale experiments," *Phys. Plasmas*, 19, pp. 062706, (2012).
[6] Chirkov, A.Yu. and Ryzhkov, S.V., "The plasma jet/laser driven compression of compact plasmoids to fusion conditions," *J. Fus. Energy*, 31(1), pp. 7-12, (2012).
[7] Mozgovoy, A.G., Romadanov, I.V. and Ryzhkov, S.V., "Formation of a compact toroid for enhanced efficiency," *Physics of Plasmas*, 21, pp. 022501-5, (2014).
[8] Grishin, S.D., Leskov, L.V. and Kozlov, N.P., *Plasma accelerators,* Moscow: Mashinostroenie, (1983). (in Russian)
[9] Morozov, A.I. and Shubin, A.P., "Plasma accelerators," *Itogy nauky i techniky. Ser. Plasma Physics*, 5, Moscow: Atomizdat, pp. 178-260, (1984). (in Russian)
[10] Kozlov, N.P. and Morozov, A.I. *Plasma accelerators and ion injectors*, Moscow: Nauka, (1984). (in Russian)
[11] Cassibry, J.T. Cortez, R.J. Hsu, S.C. and Witherspoon, F.D., "Estimates of dwell time for plasma liner driven magneto-inertial fusion using an analytic self-similar converging shock model," *Phys. Plasmas*, 16, pp. 112707, (2009).
[12] Morozov, A.I., *Introduction to Plasmodynamics*, Moscow: Fizmatlit, (2008). (in Russian)
[13] Kolesnikov, P.M., *Electrodynamic Aacceleration of Plasma*, Moscow: Atomizdat, (1971). (in Russian)
[14] Kolesnikov, P.M., *Zh. Tekh. Fiz.*, 36, pp. 80-84 (1966). [*Sov. Tech. Phys.*, 10, pp. 1219, (1966)].
[15] Zhukov, B.G., Reznikov, B.I., Kurakin, R.O. and Rozov, S.I., "Influence of the Gas Density on the Motion of a Free Plasma Piston in the Railgun Channel," *Zh. Tekh. Fiz.,* 77 (7), pp. 43-49, (2007) [*Sov. Tech. Phys.*, 52, pp. 865, (2007)].
[16] D'yakov, B.V. and Reznikov, B.I., "Influence of erosion and ablation on electrodynamic acceleration," *Zh. Tekh. Fiz.*, 58, pp. 136-143, (1988).
[17] Stanyukovich, K.P., *Unsteady motion of continuous*, London/Oxford/Paris/New York: Pergamon Press, (1960).
[18] Merzhievskii, L.A., Titov, V.M., Fadeenko, Yu.I. and Shvetsov, G.A., "High-speed launching of solid bodies," *Combustion Explosion and Shock Waves USSR*, 23(5), pp. 576-589, (1987).
[19] D'yakov, B.V. and Reznikov, B.I., *Preprint Ioffe Physicotechnical Institute*, № 969, 39 p., (1985). (in Russian)
[20] Hawke, R.S., Brooks, A.L., Fowler, K.M. and Peterson, D.R., "Electromagnetic Railgun Launchers," AIAA/JSASS/DGLR 15th International Electric Propulsion Conference, AIAA-81-0751, (1981).
[21] Hawke, R.S., *Atomkernenergie und Kerntechnik*, Bd 38, H1.S, pp. 35-46, (1981).
[22] Kuzenov, V.V. and Ryzhkov, S.V., "Developing the numerical model for studying laser-compression of magnetized plasmas," *Acta Technica,* 56, pp. T454-467, (2011).
[23] Kuzenov, V.V., Surzhikov, S.T. and Petrusev, A.S., Radiation Gas Dynamics of Aluminium Laser Plume in Air," 46th AIAA Aerospace Sciences Meeting and Exhibit, AIAA 2008-1108, (2008).
[24] Kuzenov, V.V. and Ryzhkov, S.V., "Numerical modeling of magnetized plasma compressed by the laser beams and plasma jets," *Probl. Atom. Sci. Tech.*, 1(83), pp. 12-14, (2013).
[25] Kuzenov, V.V. and Ryzhkov, S.V., "Evaluation of hydrodynamic instabilities in inertial confinement fusion target in a magnetic field," *Probl. Atom. Sci. Tech.*, 4(86), pp. 103-107, (2013).